ERJ Express. Published on February 28, 2019 as doi: 10.1183/13993003.02188-2018

EUROPEAN RESPIRATORY *journal*

FLAGSHIP SCIENTIFIC JOURNAL OF ERS

Early View

Original article

Hyperpolarised ^{129}Xe MRI to monitor treatment response in children with cystic fibrosis

Jonathan H. Rayment, Marcus J. Couch, Nancy McDonald, Nikhil Kanhere, David Manson, Giles Santyr, Felix Ratjen

Please cite this article as: Rayment JH, Couch MJ, McDonald N, *et al*. Hyperpolarised ^{129}Xe MRI to monitor treatment response in children with cystic fibrosis. *Eur Respir J* 2019; in press (https://doi.org/10.1183/13993003.02188-2018).

Hyperpolarised ^{129}Xe MRI to monitor treatment response in children with cystic fibrosis

Jonathan H Rayment[1,2,3], Marcus J Couch[3,5], Nancy McDonald[1,3], Nikhil Kanhere[3], David Manson[4], Giles Santyr[3,5] and Felix Ratjen[1,2,3]

[1] Division of Respiratory Medicine, Department of Paediatrics, Hospital for Sick Children, Toronto ON, Canada
[2] Department of Paediatrics, University of Toronto, Toronto ON, Canada.
[3] Translational Medicine Program, SickKids Research Institute, Toronto ON, Canada
[4] Department of Diagnostic Imaging, Hospital for Sick Children, Toronto ON, Canada
[5] Department of Medical Biophysics, University of Toronto, Toronto ON, Canada

Corresponding author/requests for reprints:
Jonathan H Rayment
Division of Respiratory Medicine
BC Children's Hospital
4480 Oak St
Vancouver, BC, Canada, V6H 3N1
jonathan.rayment@bcchr.ca

Running title: XeMRI CF treatment response

Key words: MRI, hyperpolarised xenon, cystic fibrosis, outcome measure, pulmonary exacerbation, treatment response

Funding:
This study was funded by The Irwin Fund and a Canadian Institutes for Health Research Project grant #376120. JHR was funded by a Cystic Fibrosis Canada clinical fellowship and MJC was supported by a MITACS Elevate award.

Competing Interests: All authors have no competing interests to declare.
Authorship statement: All authors have contributed significantly to the work, have participated in drafting or critically revising the manuscript, have seen and approved the final version of the manuscript, and take responsibility for the content of the manuscript.

Abstract

Pulmonary magnetic resonance imaging using hyperpolarised ^{129}Xe gas (XeMRI) can quantify ventilation inhomogeneity by measuring the percentage of unventilated lung volume (ventilation defect percent; VDP). While previous studies have demonstrated its sensitivity to detect early cystic fibrosis (CF) lung disease, the utility of XeMRI to monitor response to therapy in CF is unknown. The aim of this study was to assess the ability of XeMRI to capture treatment response in paediatric CF patients undergoing inpatient antibiotic treatment for a pulmonary exacerbation.

15 CF patients age 8-18 years underwent XeMRI, spirometry, plethysmography, and multiple breath nitrogen washout at the beginning and end of inpatient treatment of a pulmonary exacerbation. VDP was calculated from XeMRI images obtained during a static breath hold using semi-automated k-means clustering and linear binning approaches.

XeMRI was well tolerated. VDP, lung clearance index and the forced expiratory volume in one second all improved with treatment, however, response was not uniform in individual patients. Of all outcome measures, VDP showed the largest relative improvement (-42.1%; 95%CI -52.1, -31.9, $p<0.0001$).

These data support further investigation of XeMRI as a tool to capture treatment response in CF lung disease.

Introduction

Overall survival and lung function have improved dramatically over the past decades in patients with cystic fibrosis (CF) (1) and traditional pulmonary function tests (PFTs) such as spirometry are now often normal in the paediatric age range (2). Given this, the use of spirometric indices as endpoints in clinical trials or for the monitoring of individual response to therapy, especially in the paediatric population, can be problematic (3). The lung clearance index (LCI), an outcome measure generated from the multiple breath washout (MBW) test, reflects ventilation inhomogeneity (4, 5) and has been demonstrated to be more sensitive than spirometry to detect and monitor early lung disease in paediatric CF patients (6-8). Despite its higher sensitivity, MBW testing provides only a whole-lung assessment of ventilation inhomogeneity and imaging-based measures of lung function may be better suited to provide insight into the regional nature of disease and to detect subtle, regional pathology.

Hyperpolarised noble gas functional pulmonary magnetic resonance imaging (MRI) has shown considerable advancement over the past decade for the quantification of regional ventilation defects (9), alveolar-capillary gas diffusion (10) and pulmonary microarchitecture (11). While ^{3}He was previously the most commonly used inhaled contrast agent in this field, more centres are now using hyperpolarised ^{129}Xe for functional pulmonary MRI (XeMRI) due to the lower cost and higher availability of ^{129}Xe as well as advances in hyperpolarization physics that have allowed for greater polarization efficiency of this gas (12). The most validated hyperpolarised gas MRI technique is static ventilation imaging, which allows for the quantification of ventilation "defects" as a percentage of the total thoracic volume during a breath-hold, or ventilation defect percent (VDP). VDP can be determined using a variety of analytic techniques (9, 13, 14) and has been demonstrated to be more sensitive than spirometry at identifying lung disease in paediatric CF patients (13, 15-17). In addition, VDP appears to be more sensitive than spirometry and MBW at detecting longitudinal progression of CF lung disease (18). However, high sensitivity of a test does not necessarily imply responsiveness of that test to treatment. Previous studies using ^{3}He MRI (HeMRI) outcomes in interventional settings in CF have demonstrated treatment responsiveness of this technique (19-21). However, to date no studies have investigated the ability of XeMRI to assess the efficacy of a therapeutic intervention in the CF population. If this imaging modality is to be used to direct clinical care or as an outcome measure in clinical trials, its ability to detect response to treatment be further characterised.

In this study, we used a common clinical scenario in CF, where improvement with treatment is expected, to assess whether XeMRI can detect a treatment response. We performed XeMRI and physiological

(spirometry, plethysmography and MBW) testing on children with CF admitted to hospital for treatment of a pulmonary exacerbation before and after treatment. We used this known treatment paradigm to determine 1/ whether XeMRI is safe and feasible in a sicker population of paediatric CF patients, 2/ if XeMRI can detect changes in regional ventilation distribution following this treatment and 3/ how changes in VDP correlate with changes in spirometric and MBW outcome measures.

Methods

Patient Population

Patients with CF between the ages of 8 and 18 years, admitted to hospital for intravenous antibiotic treatment of a physician-diagnosed pulmonary exacerbation were eligible. Exclusion criteria were inability to perform PFTs or MRI, pregnancy, supplemental oxygen use or a FEV1<40% at the time of screening. Local ethics board and Health Canada approval was obtained (SickKids REB #1000049033). The study was registered at clinicaltrials.gov (NCT02606487). The responsible physician determined the treatment regimen. Healthy controls were recruited as part of a separate study (SickKids REB #1000048243, clinicaltrials.gov NCT02740868).

Study Protocol

On the day of testing, inhaled medications were held until testing was complete. Akron pulmonary exacerbation severity (APES) scores were assessed at the time of recruitment (22). A Likert scale of wellness (1-10) was collected before and after treatment. PFTs, MBW and MRI were performed on the same day within 48 hours of the initiation and completion of antibiotic treatment. Spirometry and plethysmography were performed according to ATS/ERS standards (23, 24). Nitrogen MBW testing was performed on the Exhalyzer D (Ecomedics, Dürnten, SUI) in supine and seated postures, according to standard quality control criteria (5, 25).

Hyperpolarised ^{129}Xe gas was generated as described (Model 9800, Polarean, Durham, NC, USA) and was dosed at 10% of the participant's total lung capacity, diluted in ultra high purity nitrogen to a total volume of 1L for each dose as previously described (26). XeMRI and conventional proton images were acquired at 3T (Siemens Prisma, Erlangen, Germany) in the coronal plane using a flexible vest radiofrequency coil (for XeMRI images; Clinical MR Solutions, Brookfield, Wisconsin) or a flexible torso array and spine coil (for proton images; Siemens, Erlangen, Germany). The detailed MRI protocol is described in the Online Supplement.

Image analysis

Seven slices from each image set (the center slice plus three flanking slices) were chosen for VDP analysis. XeMRI and proton MRI images were aligned using a semiautomated segmentation approach (26). VDP was calculated using two approaches: the k-means clustering approach described by Kirby and colleagues (9) and the mean-anchored, linear binning approach described by Collier and colleagues (27). The VDP

threshold in the linear binning technique was estimated from the mean signal intensity distribution of the ten healthy controls (see online supplement).

Statistical Analysis

Statistical analyses were performed using STATA v14 (Stata Corp., College Station, TX, USA). Within-subject absolute changes in outcome measures were post-treatment values minus the pre-treatment values. Within-subject relative changes were the absolute changes divided by the pre-treatment values. Within-subject absolute and relative outcome measures changes are reported with 95% confidence intervals. Correlation of outcome measures was assessed with simple linear regression and the coefficient of determination (R^2) is reported.

Results

Patient population

Between December 2016 and August 2017, 33 children with CF between 8 and 18 years of age admitted to the Hospital for Sick Children for treatment of a pulmonary exacerbation were screened, 20 were enrolled and 15 completed the study (Figure 1). Of the enrolled subjects, one could not perform MBW testing, one was unable to correctly complete the breath-hold manoeuvre for XeMRI and three had their diagnoses of pulmonary exacerbation revised by their treating physicians and were discharged from hospital prior to completing a full course of antibiotic therapy. Data from the 15 participants who completed the study were included in the final analysis and their characteristics are shown in Table 1. The median age was 14 years, and baseline lung function was relatively preserved, with a median best FEV_1 in the 6 months preceding the pulmonary exacerbation of 85.0% (IQR 61.0, 93.0).

At the time of admission, the median APES was 11.0 (IQR 8.0, 14.0). Mean FEV_1 at the time of admission was 62.9% (13.9), which represented a median relative drop of 18.0% (IQR -8.0, -31.0) from baseline (best FEV_1 in the past 6 months). Antibiotic treatment duration was 13 or 14 days for 14/15 participants and 22 days for one participant.

^{129}Xe MRI Tolerability and feasibility

The gas dosing volumes used in this study, as a fraction of total lung capacity, are shown in Table S1. All test procedures were well tolerated. Transient, self-resolving oxygen desaturations (SpO2<88% lasting up to 10 seconds) were observed in 15/30 (50%) XeMRI scans. The median oxygen saturation nadir for all scans was 88% (IQR 81-91). No desaturations lasted longer than 10 seconds and no scans were aborted due to adverse events. Analyzable images were acquired in all but one scanned participant. Representative ventilation defect maps generated using the k-means and linear binning techniques and the corresponding signal histogram are shown in Figure 2.

Imaging and physiology responses to antibiotic treatment

Imaging, spirometric, plethysmographic, MBW and symptom score outcomes all improved significantly following treatment (Table 2). VDP (calculated using the linear binning technique) showed the greatest mean relative improvement of all outcome measures (-42.1%; 95%CI -57.3, -26.8, p<0.0001), dropping from a mean of 6.8% to 3.8%. In most participants, the distribution of XeMRI ventilation signal intensity

shifted towards the healthy range (see Figure S1 for the derivation of the healthy distribution) but did not completely return to a healthy distribution in any case (Figure S2, Online Data Supplement). Seated LCI showed a significant mean improvement following treatment (-9.1%; 95%CI -15.5, -2.6; p=0.009), but there was no overall change observed in supine LCI (-2.7%; 95%CI -9.6, 4.2; p=0.4). The distribution of individual relative changes in imaging and physiologic outcomes is shown in Figure 3. Absolute FEV_1 and LCI values correlated with VDP (Table S2). However, there was no correlation between the magnitude of change of the imaging and physiologic outcomes

Unprocessed XeMRI data, signal intensity histograms and physiologic data are shown from three cases that exemplify the complementarity of the data obtained using the techniques (Figure 4). In example 1 (Figure 4A), there was an improvement in FEV_1, LCI and VDP. Qualitative analysis of the XeMRI signal histogram generated by the linear binning technique demonstrated resolution of a low-intensity signal plateau seen at the left half of the histogram. In example 2 (Figure 4B), treatment resulted in an increase in FEV_1, while the LCI and VDP worsened. Qualitative assessment of the XeMRI signal histogram showed a distinct distribution pattern with a very high frequency of lower intensity signal (suggesting widespread regions of poorly ventilated lung) that did not change substantially with treatment. Finally, in example 3 (Figure 4C) the FEV_1 did not improve following treatment, but both VDP and LCI decreased, and the post-treatment XeMRI signal intensity histogram shifted towards the normal range with reductions in focal defects on the XeMRI images.

Discussion

In this study, we assessed the ability of hyperpolarised ^{129}Xe pulmonary MRI (XeMRI) to detect changes in ventilation distribution following inpatient treatment of a CF pulmonary exacerbation. The study procedure was well tolerated in all cases. We demonstrate responsiveness of this outcome measure, reflected by a significant decrease in poorly ventilated lung (quantified by VDP) following treatment. The change in VDP signal was substantial, with a relative improvement of approximately 40%, suggesting that this technique can generate outcomes that are robustly responsive to treatment regardless of the image analysis technique that is used. Importantly, the change in VDP did not correlate with changes in MBW or spirometry outcomes, suggesting that these modalities provide complementary information.

To our knowledge, this is the largest study to investigate hyperpolarised gas functional pulmonary MRI as a tool to monitor treatment response in CF, and the first using XeMRI. One other study has assessed the ability of hyperpolarised HeMRI to detect a treatment response to a pharmacologic intervention. In a double-blind study of 8 CF patients with gating mutations, Altes and colleagues demonstrated that HeMRI can identify a decrease in ventilation defects after treatment with ivacaftor, a CFTR modulator (19). Additionally, previous HeMRI studies failed to demonstrate a net treatment response to airway clearance therapies using global ventilation defect measures, though the location of the defects changed with treatment (20, 21). Advanced regional XeMRI image analysis techniques (28) may be able to provide a more detailed physiologic quantification of treatment responsiveness, however data from the ivacaftor study and the current trial suggest that global hyperpolarised gas MRI measures like VDP are responsive to changes in pulmonary ventilation distribution following treatment in CF. More evidence in the interventional setting is needed to define how responsive this technique is to treatment, compared to other available testing modalities.

Another potential clinical role for hyperpolarised gas MRI may be in longitudinal monitoring of CF lung disease. The rate of FEV_1 decline in CF is low, even in adulthood (29) and spirometry is typically stably normal in younger children (30). Techniques such as MBW are more sensitive than spirometry to detect the progression of lung disease over time in young children (30), but recent data have suggested that HeMRI (and VDP in particular) may be even more sensitive than MBW at detecting the longitudinal progression of disease (18). Especially in the era of CFTR modulators where we expect the annual rate of lung function decline to be further diminished (or potentially halted) (31), highly sensitive tools to monitor lung function progression over time will become increasingly important to clinical care.

In this study, we confirmed correlation between VDP and both LCI and FEV_1 (15, 17). However, the correlation of VDP and LCI was weaker in the current study than previously observed. This could be due to the fact that the participants in this study had more severe lung disease , with lower FEV_1 and higher LCI than our group's previous assessment of stable CF participants (15). Additionally these children were also suffering from an acute pulmonary exacerbation. These differences could result in higher variability of measures of ventilation inhomogeneity (32, 33). Contrastingly, a recent study by Smith and colleagues (17) interrogating regional physiology in children with CF using HeMRI and MBW techniques showed good correlation between VDP and LCI even in those with worse lung function. However, in this same paper, the authors also demonstrated that as imaged lung volume approached total lung capacity (TLC), measured VDP decreased. Measurements in this study were obtained at a lung volume corresponding to approximately 80% of TLC (see Table S1), which is lower than the 60% of TLC that was targeted by Smith and colleagues. It is therefore possible that imaging at a higher lung volume introduced a "ceiling effect" and that VDP was relatively underestimated, especially in smaller patients, thereby decreasing imaging-physiology correlation. This same phenomenon may also have blunted the observed magnitude of treatment response. Gas contrast dosing in future studies should based on subject lung volumes in order to minimise this potential confounding effect.

Interestingly, while the absolute physiologic and imaging outcome measures were correlated, the magnitude of changes in VDP did not correlate with changes in LCI or FEV1, suggesting that these measures are providing complementary information about treatment response. Examples of individual cases with conflicting results for spirometry, MBW and XeMRI results (Figure 4) demonstrate the complementary nature of these tests. Future studies should to assess the relationship and combined utility of XeMRI-derived and physiologic outcome measures in predicting long-term outcomes and/or disease progression to better define which measurement(s) should be used to best guide treatment decisions.

Somewhat surprisingly, we found that VDP correlated slightly better with seated MBW outcomes (see Table S3, Online Data Supplement) than those collected in the supine posture (the posture in which the MRI was performed). This is contrary to recent data that have shown that structural CT scores correlate better with MBW taken in the supine posture (34), though Smith and colleagues also observed slightly better correlation of VDP with seated LCI in their recent paper (17). The aetiology of this observation is not entirely clear but may again be related to the lung volume at which the XeMRI images were obtained. While the supine posture reduces resting lung volume, performing imaging above FRC likely shifts the imaged lung volumes closer to those seen in the sitting position.

One final observation of this study was the impact of disease stability on the postural dependence of MBW outcomes. There is existing evidence that the posture in which MBW testing is performed influences the outcome measures that are generated, with ventilation heterogeneity increasing in the supine posture (35, 36). We confirmed this finding in the current study, showing that the LCI was significantly higher and the FRC significantly lower in a supine posture than in a seated posture. However, this postural dependence of MBW outcomes is diminished (or in the case of LCI, completely abolished) in the pre-treatment participants, but is recovered following therapy (see Table S2, Online Data Supplement). These are similar to Smith and colleagues' observation (35) that children with CF had less predictable posture-driven changes in MBW outcomes than those with no lung disease. We hypothesise that mucous plugs, which are a major radiographic feature of CF patients suffering from an exacerbation (37, 38), may shift unpredictably with postural changes leading to less predictable changes in regional ventilation patterns in sicker patients as they change postures.

Strengths of this study include its prospective design, and the same-day measurement of multiple outcome measures including a standardized approach to the collection and analysis of XeMRI data. The primary limitation of this study is that the intervention studied is not necessarily a scenario in which XeMRI is likely to be used clinically. Similar to what has been done for other outcome measures, pulmonary exacerbations were chosen as a first step of evaluation because of a predictable improvement following treatment in most outcome measures on a group level (39). Now that XeMRI has been shown to be responsive to treatment in this setting, future studies can assess its responsiveness to other interventions in which smaller signals in traditional pulmonary function tests are typically seen (7, 40). Additionally, structural analysis was not performed in this study. Significant advancements in traditional proton MRI techniques have also been able to demonstrate responses in structural and perfusion scores following therapeutic interventions in CF, though this responsiveness is variable (37, 41, 42). The combination of structural and functional MRI techniques will provide important future insights into CF disease mechanisms and treatment responsiveness (43) and should be considered in future studies investigating treatment responsiveness of MRI techniques. Finally, in contrast to current structural MRI techniques (41), the XeMRI performed in this study was limited to participants who were capable of performing an adequate breath hold manoeuvre. While one study has demonstrated some success in free-breathing infants with HeMRI (44), this remains a significant drawback of this technique.

In conclusion, this study has shown that that XeMRI is responsive to treatment of pulmonary exacerbations in paediatric CF participants, with a robust decreases observed in VDP. This demonstrates that XeMRI shows promise as an emerging imaging biomarker for monitoring treatment response in CF. In addition,

XeMRI has a potential role as a research tool to better understand the complex and spatially heterogenous pathophysiology of CF lung disease.

References

1. Stephenson AL, Sykes J, Stanojevic S, Quon BS, Marshall BC, Petren K, Ostrenga J, Fink AK, Elbert A, Goss CH. Survival Comparison of Patients With Cystic Fibrosis in Canada and the United States: A Population-Based Cohort Study. *Ann Intern Med* 2017; 166: 537-546.
2. Marshall B, Faro A, Elbert A, Fink A, Sewall A, Loeffler D, Petren K, O'Neil T, Rizvi S. Cystic Fibrosis Foundation Patient Registry 2016 Annual Data Report. Bethesda, MD, USA; 2017.
3. Stanojevic S, Ratjen F. Physiologic endpoints for clinical studies for cystic fibrosis. *J Cyst Fibros* 2016; 15: 416-423.
4. Robinson PD, Goldman MD, Gustafsson PM. Inert gas washout: theoretical background and clinical utility in respiratory disease. *Respiration* 2009; 78: 339-355.
5. Robinson PD, Latzin P, Verbanck S, Hall GL, Horsley A, Gappa M, Thamrin C, Arets HG, Aurora P, Fuchs SI, King GG, Lum S, Macleod K, Paiva M, Pillow JJ, Ranganathan S, Ratjen F, Singer F, Sonnappa S, Stocks J, Subbarao P, Thompson BR, Gustafsson PM. Consensus statement for inert gas washout measurement using multiple- and single- breath tests. *Eur Respir J* 2013; 41: 507-522.
6. Aurora P, Bush A, Gustafsson P, Oliver C, Wallis C, Price J, Stroobant J, Carr S, Stocks J. Multiple-breath washout as a marker of lung disease in preschool children with cystic fibrosis. *Am J Respir Crit Care Med* 2005; 171: 249-256.
7. Ratjen F, Hug C, Marigowda G, Tian S, Huang X, Stanojevic S, Milla CE, Robinson PD, Waltz D, Davies JC. Efficacy and safety of lumacaftor and ivacaftor in patients aged 6-11 years with cystic fibrosis homozygous for F508del-CFTR: a randomised, placebo-controlled phase 3 trial. *Lancet Respir Med* 2017; 5: 557-567.
8. Rayment JH, Stanojevic S, Davis SD, Retsch-Bogart G, Ratjen F. Lung clearance index to monitor treatment response in pulmonary exacerbations in preschool children with cystic fibrosis. *Thorax* 2018; 73: 451-458.
9. Kirby M, Svenningsen S, Ahmed H, Wheatley A, Etemad-Rezai R, Paterson NA, Parraga G. Quantitative evaluation of hyperpolarized helium-3 magnetic resonance imaging of lung function variability in cystic fibrosis. *Acad Radiol* 2011; 18: 1006-1013.
10. Driehuys B, Cofer GP, Pollaro J, Mackel JB, Hedlund LW, Johnson GA. Imaging alveolar-capillary gas transfer using hyperpolarized 129Xe MRI. *Proc Natl Acad Sci U S A* 2006; 103: 18278-18283.
11. Saam BT, Yablonskiy DA, Kodibagkar VD, Leawoods JC, Gierada DS, Cooper JD, Lefrak SS, Conradi MS. MR imaging of diffusion of (3)He gas in healthy and diseased lungs. *Magn Reson Med* 2000; 44: 174-179.
12. Mugler JP, Altes TA. Hyperpolarized 129Xe MRI of the human lung. *J Magn Reson Imaging* 2013; 37: 313-331.
13. Thomen RP, Walkup LL, Roach DJ, Cleveland ZI, Clancy JP, Woods JC. Hyperpolarized 129Xe for investigation of mild cystic fibrosis lung disease in pediatric patients. *J Cyst Fibros* 2017; 16: 275-282.
14. He M, Driehuys B, Que LG, Huang YT. Using Hyperpolarized 129Xe MRI to Quantify the Pulmonary Ventilation Distribution. *Acad Radiol* 2016; 23: 1521-1531.
15. Kanhere N, Couch MJ, Kowalik K, Zanette B, Rayment JH, Manson D, Subbarao P, Ratjen F, Santyr G. Correlation of Lung Clearance Index with Hyperpolarized 129Xe Magnetic Resonance Imaging in Pediatric Subjects with Cystic Fibrosis. *Am J Respir Crit Care Med* 2017; 196: 1073-1075.
16. Marshall H, Horsley A, Taylor CJ, Smith L, Hughes D, Horn FC, Swift AJ, Parra-Robles J, Hughes PJ, Norquay G, Stewart NJ, Collier GJ, Teare D, Cunningham S, Aldag I, Wild JM. Detection of early subclinical lung disease in children with cystic fibrosis by lung ventilation imaging with hyperpolarised gas MRI. *Thorax* 2017; 72: 760-762.

17. Smith LJ, Collier GJ, Marshall H, Hughes PJC, Biancardi AM, Wildman M, Aldag I, West N, Horsley A, Wild JM. Patterns of regional lung physiology in cystic fibrosis using ventilation magnetic resonance imaging and multiple-breath washout. *Eur Respir J* 2018; 52.
18. Smith L, Marshall H, Aldag I, Horn F, Collier G, Hughes D, West N, Horsley A, Taylor CJ, Wild J. Longitudinal Assessment of Children with Mild Cystic Fibrosis Using Hyperpolarized Gas Lung Magnetic Resonance Imaging and Lung Clearance Index. *Am J Respir Crit Care Med* 2018; 197: 397-400.
19. Altes TA, Johnson M, Fidler M, Botfield M, Tustison NJ, Leiva-Salinas C, de Lange EE, Froh D, Mugler JP. Use of hyperpolarized helium-3 MRI to assess response to ivacaftor treatment in patients with cystic fibrosis. *J Cyst Fibros* 2017; 16: 267-274.
20. Bannier E, Cieslar K, Mosbah K, Aubert F, Duboeuf F, Salhi Z, Gaillard S, Berthezène Y, Crémillieux Y, Reix P. Hyperpolarized 3He MR for sensitive imaging of ventilation function and treatment efficiency in young cystic fibrosis patients with normal lung function. *Radiology* 2010; 255: 225-232.
21. Mentore K, Froh DK, de Lange EE, Brookeman JR, Paget-Brown AO, Altes TA. Hyperpolarized HHe 3 MRI of the lung in cystic fibrosis: assessment at baseline and after bronchodilator and airway clearance treatment. *Acad Radiol* 2005; 12: 1423-1429.
22. Kraynack NC, McBride JT. Improving care at cystic fibrosis centers through quality improvement. *Semin Respir Crit Care Med* 2009; 30: 547-558.
23. Miller MR, Hankinson J, Brusasco V, Burgos F, Casaburi R, Coates A, Crapo R, Enright P, van der Grinten CP, Gustafsson P, Jensen R, Johnson DC, MacIntyre N, McKay R, Navajas D, Pedersen OF, Pellegrino R, Viegi G, Wanger J, Force AET. Standardisation of spirometry. *Eur Respir J* 2005; 26: 319-338.
24. Wanger J, Clausen JL, Coates A, Pedersen OF, Brusasco V, Burgos F, Casaburi R, Crapo R, Enright P, van der Grinten CP, Gustafsson P, Hankinson J, Jensen R, Johnson D, Macintyre N, McKay R, Miller MR, Navajas D, Pellegrino R, Viegi G. Standardisation of the measurement of lung volumes. *Eur Respir J* 2005; 26: 511-522.
25. Jensen R, Stanojevic S, Klingel M, Pizarro ME, Hall GL, Ramsey K, Foong R, Saunders C, Robinson PD, Webster H, Hardaker K, Kane M, Ratjen F. A Systematic Approach to Multiple Breath Nitrogen Washout Test Quality. *PLoS One* 2016; 11: e0157523.
26. Santyr G, Kanhere N, Morgado F, Rayment JH, Ratjen F, Couch MJ. Hyperpolarized Gas Magnetic Resonance Imaging of Pediatric Cystic Fibrosis Lung Disease. *Acad Radiol* 2018.
27. Collier J, Acunzo L, Smith L, Hughes P, Norquay G, Chan H, Biancardi A, Marshall H, JM W. Linear binning maps for image analysis of pulmonary ventilation with hyperpolarized gas MRI: transferability and clinical applications ISMRM. Paris; 2018.
28. Horn FC, Marshall H, Collier GJ, Kay R, Siddiqui S, Brightling CE, Parra-Robles J, Wild JM. Regional Ventilation Changes in the Lung: Treatment Response Mapping by Using Hyperpolarized Gas MR Imaging as a Quantitative Biomarker. *Radiology* 2017; 284: 854-861.
29. Stephenson A, Mak D, Mahmood A, Sykes J, Stanojevic S. The Canadian Cystic Fibrosis Registry 2016 Annual Data Report. Toronto: Cystic Fibrosis Canada; 2017.
30. Stanojevic S, Davis SD, Retsch-Bogart G, Webster H, Davis M, Johnson RC, Jensen R, Pizarro ME, Kane M, Clem CC, Schornick L, Subbarao P, Ratjen FA. Progression of Lung Disease in Preschool Patients with Cystic Fibrosis. *Am J Respir Crit Care Med* 2017; 195: 1216-1225.
31. Schechter MS, Regelmann WE, Sawicki GS, Rasouliyan L, VanDevanter DR, Rosenfeld M, Pasta D, Morgan W, Konstan MW. Antibiotic treatment of signs and symptoms of pulmonary exacerbations: a comparison by care site. *Pediatr Pulmonol* 2015; 50: 431-440.
32. Oude Engberink E, Ratjen F, Davis SD, Retsch-Bogart G, Amin R, Stanojevic S. Inter-test reproducibility of the lung clearance index measured by multiple breath washout. *Eur Respir J* 2017; 50.

33. Svedberg M, Gustafsson PM, Robinson PD, Rosberg M, Lindblad A. Variability of lung clearance index in clinically stable cystic fibrosis lung disease in school age children. *J Cyst Fibros* 2018; 17: 236-241.
34. Ramsey KA, Rosenow T, Turkovic L, Skoric B, Banton G, Adams AM, Simpson SJ, Murray C, Ranganathan SC, Stick SM, Hall GL. Lung Clearance Index and Structural Lung Disease on Computed Tomography in Early Cystic Fibrosis. *Am J Respir Crit Care Med* 2016; 193: 60-67.
35. Smith LJ, Macleod KA, Collier GJ, Horn FC, Sheridan H, Aldag I, Taylor CJ, Cunningham S, Wild JM, Horsley A. Supine posture changes lung volumes and increases ventilation heterogeneity in cystic fibrosis. *PLoS One* 2017; 12: e0188275.
36. Prisk GK, Elliott AR, Guy HJ, Verbanck S, Paiva M, West JB. Multiple-breath washin of helium and sulfur hexafluoride in sustained microgravity. *J Appl Physiol (1985)* 1998; 84: 244-252.
37. Stahl M, Wielputz MO, Graeber SY, Joachim C, Sommerburg O, Kauczor HU, Puderbach M, Eichinger M, Mall MA. Comparison of Lung Clearance Index and Magnetic Resonance Imaging for Assessment of Lung Disease in Children with Cystic Fibrosis. *Am J Respir Crit Care Med* 2017; 195: 349-359.
38. Davis SD, Fordham LA, Brody AS, Noah TL, Retsch-Bogart GZ, Qaqish BF, Yankaskas BC, Johnson RC, Leigh MW. Computed tomography reflects lower airway inflammation and tracks changes in early cystic fibrosis. *Am J Respir Crit Care Med* 2007; 175: 943-950.
39. Horsley AR, Davies JC, Gray RD, Macleod KA, Donovan J, Aziz ZA, Bell NJ, Rainer M, Mt-Isa S, Voase N, Dewar MH, Saunders C, Gibson JS, Parra-Leiton J, Larsen MD, Jeswiet S, Soussi S, Bakar Y, Meister MG, Tyler P, Doherty A, Hansell DM, Ashby D, Hyde SC, Gill DR, Greening AP, Porteous DJ, Innes JA, Boyd AC, Griesenbach U, Cunningham S, Alton EW. Changes in physiological, functional and structural markers of cystic fibrosis lung disease with treatment of a pulmonary exacerbation. *Thorax* 2013; 68: 532-539.
40. Milla CE, Ratjen F, Marigowda G, Liu F, Waltz D, Rosenfeld M, * V--PBIG. Lumacaftor/Ivacaftor in Patients Aged 6-11 Years with Cystic Fibrosis and Homozygous for F508del-CFTR. *Am J Respir Crit Care Med* 2017; 195: 912-920.
41. Stahl M, Wielpütz MO, Ricklefs I, Dopfer C, Barth S, Schlegtendal A, Graeber SY, Sommerburg O, Diekmann G, Hüsing J, Koerner-Rettberg C, Nährlich L, Dittrich AM, Kopp MV, Mall MA. Preventive Inhalation of Hypertonic Saline in Infants with Cystic Fibrosis (PRESIS): A Randomized, Double-Blind, Controlled Study. *Am J Respir Crit Care Med* 2018.
42. Wielputz MO, Puderbach M, Kopp-Schneider A, Stahl M, Fritzsching E, Sommerburg O, Ley S, Sumkauskaite M, Biederer J, Kauczor HU, Eichinger M, Mall MA. Magnetic resonance imaging detects changes in structure and perfusion, and response to therapy in early cystic fibrosis lung disease. *Am J Respir Crit Care Med* 2014; 189: 956-965.
43. Thomen R, Walkup L, Roach D, Higano N, Cleveland Z, Schapiro A, Brody A, Clancy J, Woods J. Investigation of Structure-Function Relationships in Cystic Fibrosis Lung Disease Using Hyperpolarized Xenon and Ultra-Short Echo MRI. Conference of the American Thoracic Society. San Diego; 2018.
44. Altes TA, Meyer CH, Mata JF, Froh DK, Paget-Brown A, Gerald Teague W, Fain SB, de Lange EE, Ruppert K, Botfield MC, Johnson MA, Mugler JP. Hyperpolarized helium-3 magnetic resonance lung imaging of non-sedated infants and young children: a proof-of-concept study. *Clin Imaging* 2017; 45: 105-110.

Tables

Table 1 – Baseline and admission characteristics of the participants (n=15). Data are shown as median (IQR) or number (%) unless otherwise specified.

Baseline Characteristics	
Age (years)	14 (13.0, 16.5)
Male sex	5 (33.3)
Height (cm)	153 (148, 163)
Weight (kg)	43.4 (38.2, 48.6)
Pancreatic insufficient	12 (80.0)
CF liver disease	1 (6.7)
Number of admissions in previous 18 months; mean (range)	1.2 (0, 5)
Baseline FEV1 (best in past 6 months)	85.0 (61.0, 93.0)
Admission Characteristics	
Akron pulmonary exacerbation score	11.0 (8.0, 14.0)
Likert wellness score (1-10 scale)	7 (5, 7)
Median relative drop in FEV1 from baseline on admission	-18.0 (-8.0, -31.0)
FEV1, mean (SD)	62.9 (13.9)
LCI (sitting), mean (SD)	15.1 (2.4)
BMI percentile	22 (4, 39)
Sputum microbiology at admission, number positive (percent)	
Methicillin sensitive *Staphylococcus aureus*	7 (46.7)
Pseudomonas aeruginosa	4 (26.7)
Achromobacter spp	3 (20.0)
Aspergillus spp	2 (13.3)
Mycobacterium abscessus	2 (13.3)

Other	5 (33.3)

Table 2 – Mean physiologic and imaging outcome measures before and after treatment. Mean within-subject absolute and relative change in these measures following treatment is also shown. * denotes a change that is significantly different from 0 ($p<0.05$). Acronyms: FRC functional residual capacity, CEV cumulative expired volume,

	Pre-treatment; mean (SD)	**Post-treatment; mean (SD)**	**Within subject absolute change; mean (95%CI)**	**Within-subject relative change (%); mean (95%CI)**
XeMRI outcomes				
VDP (%; linear binning)	6.8 (3.8)	3.8 (2.7)	-3.0 (-4.9, -1.1)*	-42.1 (-52.2, -31.9)*
VDP (%; k-means)	10.4 (4.5)	6.7 (4.1)	-3.8 (-5.9, -1.7)*	-34.6 (-49.3, -19.9)*
MBW outcomes (seated)				
LCI	15.2 (2.4)	13.7 (2.4)	-1.5 (-2.4, -0.5)*	-9.1 (-15.5, -2.6)*
FRC (L)	2.3 (0.7)	2.3 (0.7)	0.0 (-0.6, 0.6)	-2.8 (-61.1, 57.4)
CEV (L)	35.6 (15.3)	31.6 (14.1)	-4.1 (-6.7, -1.5)*	-10.7 (-16.2, -5.2)*
S_{acin} (L^{-1})	0.60 (0.38)	0.45 (0.24)	-0.16 (-0.32, 0.01)	-15.4 (-36.2, 5.3)
S_{cond} (L^{-1})	0.15 (0.07)	0.15 (0.06)	0.00 (-0.05, 0.04)	13.2 (-13.2, 39.6)
MBW outcomes (supine)				
LCI	15.4 (2.5)	14.9 (2.5)	-0.5 (-1.5, 0.5)	-2.7 (-9.6, 4.2)
FRC (L)	2.1 (0.6)	2.0 (0.6)	-0.2 (-0.8, 0.3)	-1.0 (-23.0, 30.7)
CEV (L)	33.1 (13.8)	29.9 (14.2)	-3.2 (-5.4, -1.0)*	-10.2 (-16.2, -4.2)*
S_{acin} (L^{-1})	0.61 (0.45)	0.44 (0.21)	-0.16 (-0.32, 0.01)	-15.4 (-36.2, 5.3)
S_{cond} (L^{-1})	0.18 (0.09)	0.19 (0.07)	0.00 (-0.05, 0.04)	13.2 (-13.2, 39.6)
Spirometry and plethysmography outcomes				
FEV1 (% pred)	63.0 (13.9)	80.3 (14.6)	17.4 (12.7, 22.1)*	29.8 (21.1, 38.5)*
RV/TLC	37.6 (9.6)	30.3 (4.6)	-7.8 (-11.6, -4.0)*	-17.9 (-25.2, -10.6)*
FRC (L)	2.5 (0.7)	2.4 (0.6)	-0.1 (-0.2, 0.0)*	-4.1 (-9.1, 1.0)
Clinical score outcome				

Likert wellness score (1-10), median (IQR)	7 (5, 7)	9 (7, 10)	2.0 (0.6, 3.4)*	39.1 (14.5, 63.7)*

Figure Legends

Figure 1 – Study flow diagram demonstrating screening, enrollment and study completion.

Figure 2 – Examples of XeMRI images, VDP mask overlays and a XeMRI signal intensity histogram from the same participant. (A) Unprocessed XeMRI signal; (B) Colourized proton MRI (purple) and XeMRI (green) acquisitions after registration (i.e. alignment); ventilation maps calculated using the (C) k-means and (D) linear binning techniques demonstrating ventilated (green) and unventilated (red) lung; (E) XeMRI signal intensity histogram plotting the distribution of normalized voxel intensity, with low signal intensity being shown on the left; the mean healthy intensity distribution is overlaid (hashed line) and the calculated VDP threshold is demonstrated by the vertical line.

Figure 3 – Relative improvement of LCI, FEV_1 and VDP (k-means and linear binning techniques) following treatment. Individual relative changes (100% x [pre-treatment value – post-treatment value] / pre-treatment value) are shown in hollow circles. Improvement is always depicted as a positive change regardless of the nature of the outcome measure. No change is indicated by the dashed horizontal line. The mean relative change and 95% confidence intervals are shown.

Figure 4 – XeMRI ventilation images (3 slices shown) and signal intensity histograms before and after treatment for (a) participant 20 (b) participant 9 and (c) participant 13. For the signal intensity histograms, pre-treatment distribution is shown in dark grey and post-treatment distribution is shown in white. The mean healthy distribution is overlaid in a hashed curve and the calculated ventilation defect threshold is identified with a dashed vertical line.

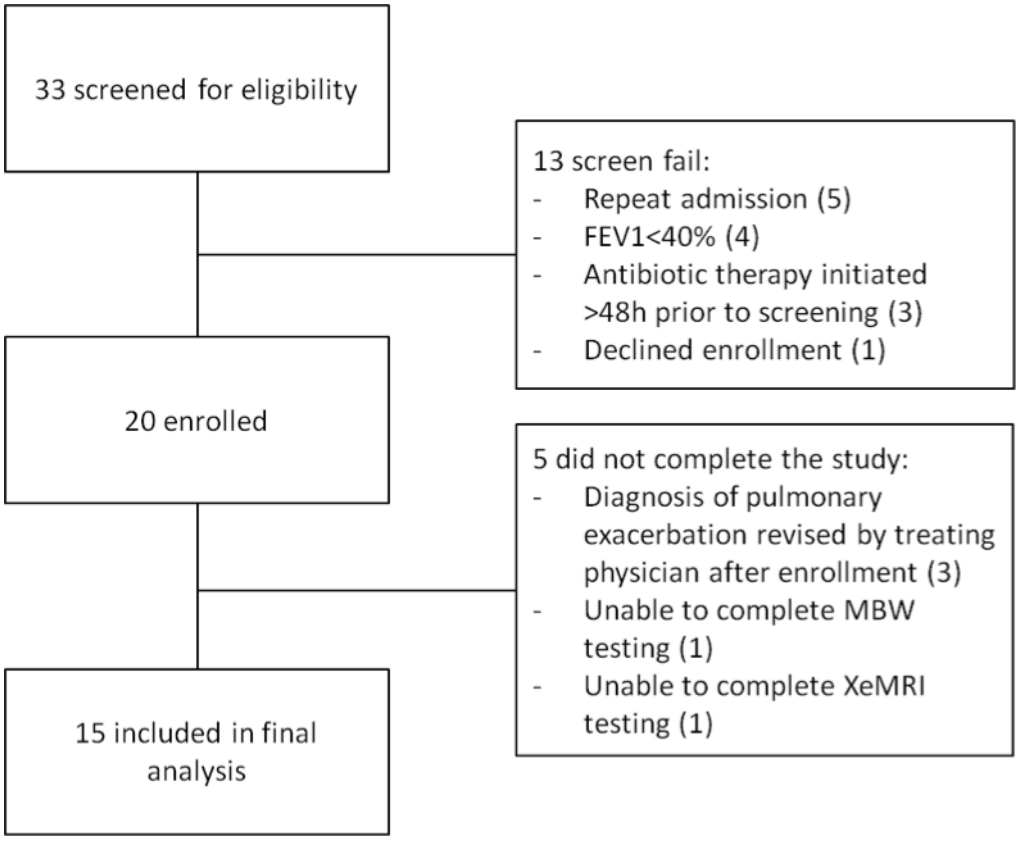
33 screened for eligibility
13 screen fail:
- Repeat admission (5)
- FEV1<40% (4)
- Antibiotic therapy initiated >48h prior to screening (3)
- Declined enrollment (1)
20 enrolled
5 did not complete the study:
- Diagnosis of pulmonary exacerbation revised by treating physician after enrollment (3)
- Unable to complete MBW testing (1)
- Unable to complete XeMRI testing (1)
15 included in final analysis

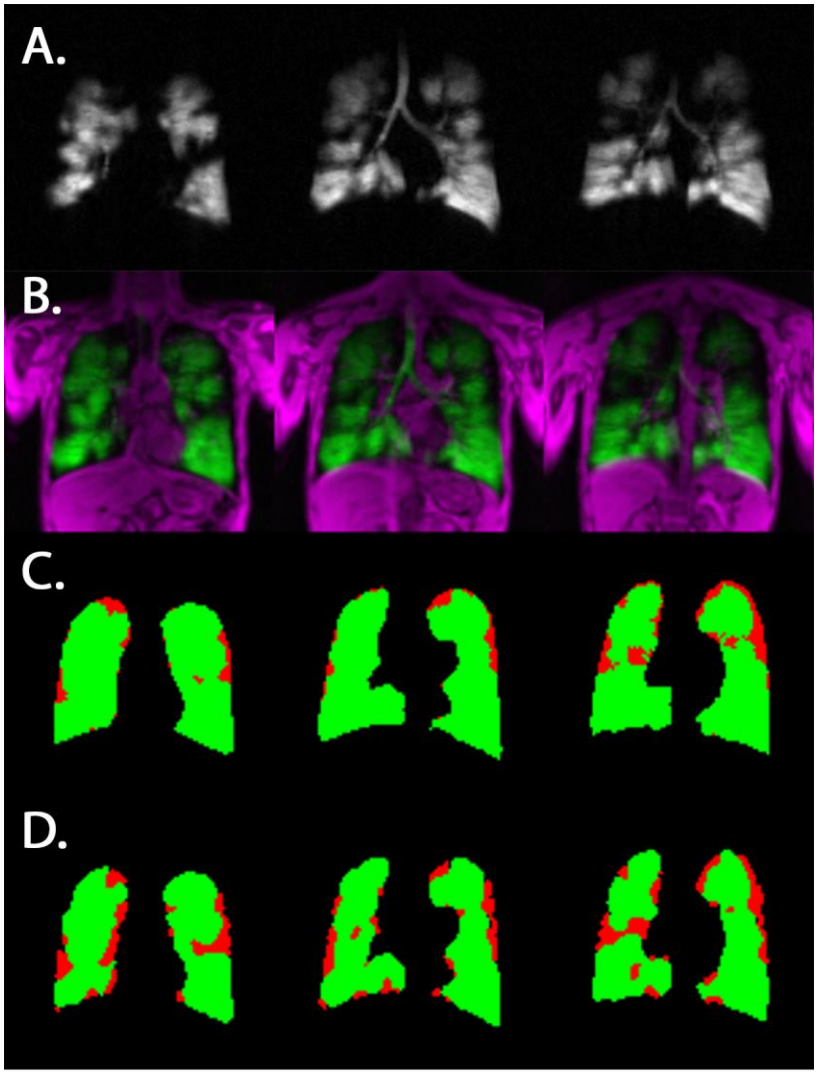
A.
B.
C.
D.

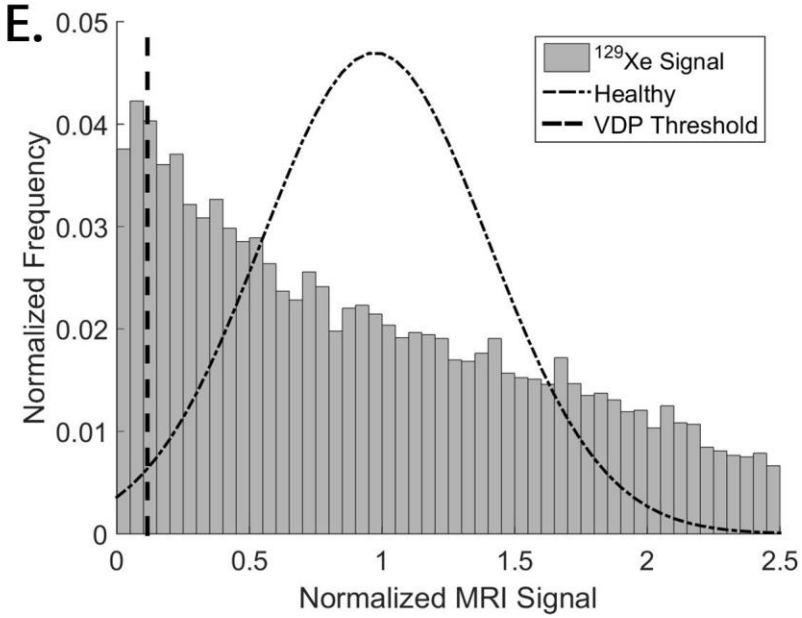
E.
0.05
0.04
0.03
0.02
0.01
0
Normalized Frequency
0
0.5
1
1.5
2
2.5
Normalized MRI Signal
129Xe Signal
Healthy
VDP Threshold

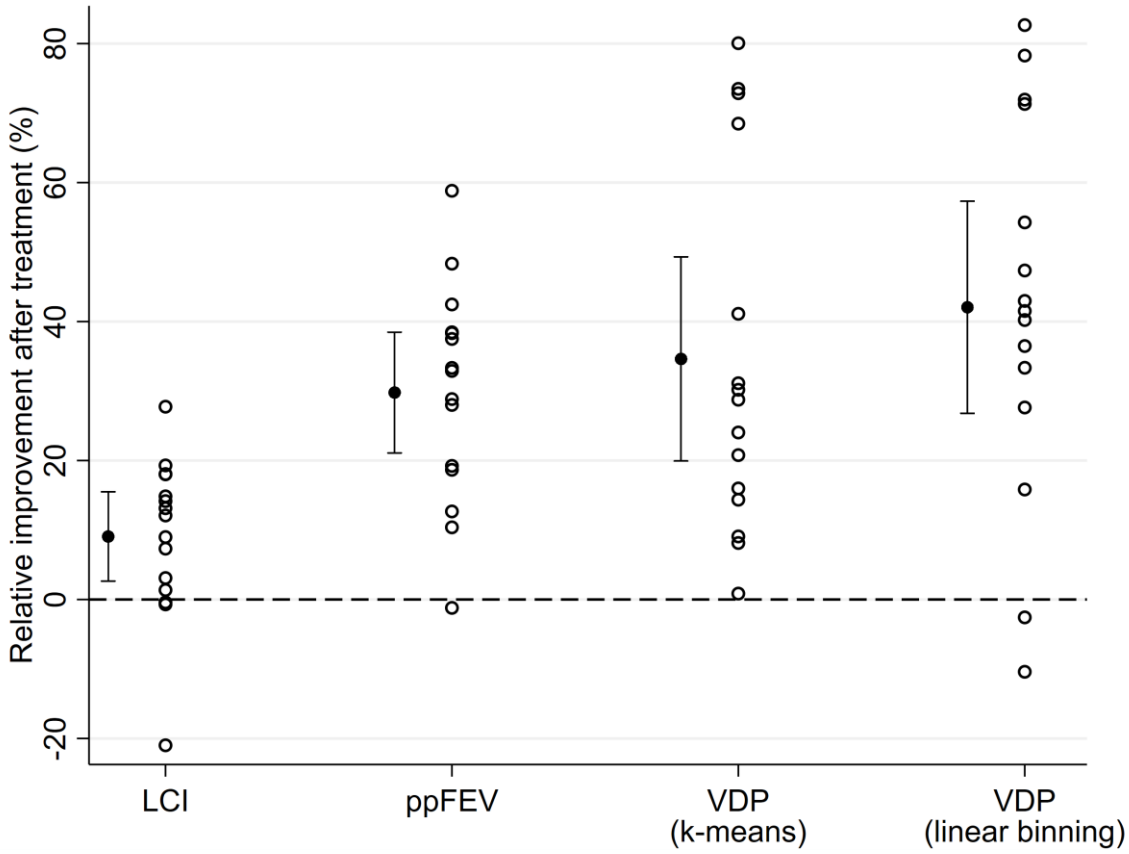
Relative improvement after treatment (%)
-20
0
20
40
60
80
LCI
ppFEV
VDP
(k-means)
VDP
(linear binning)

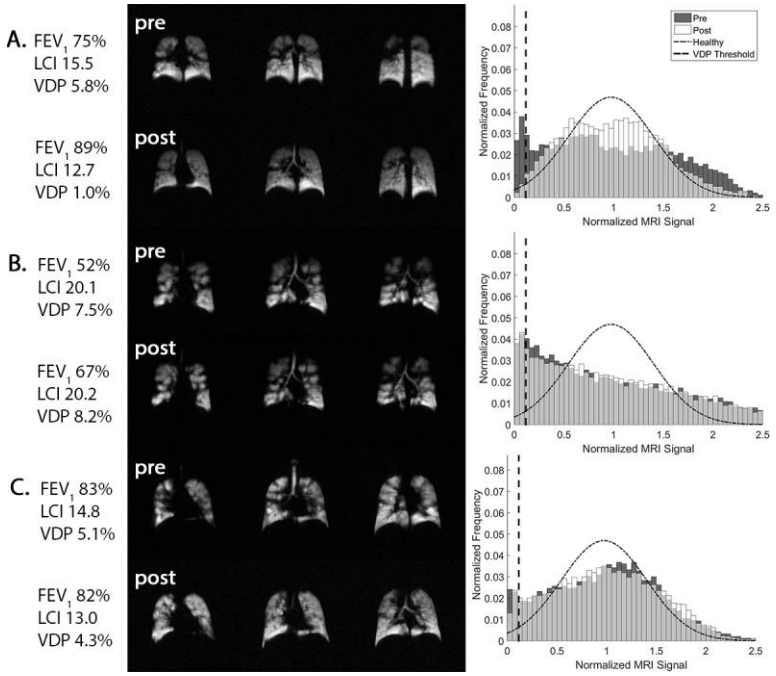
A. FEV1 75%
LCI 15.5
VDP 5.8%
pre
FEV1 89%
LCI 12.7
VDP 1.0%
post
B. FEV1 52%
LCI 20.1
VDP 7.5%
pre
FEV1 67%
LCI 20.2
VDP 8.2%
post
C. FEV1 83%
LCI 14.8
VDP 5.1%
pre
FEV1 82%
LCI 13.0
VDP 4.3%
post
Pre
Post
Healthy
VDP Threshold
Normalized Frequency
Normalized MRI Signal

Online Data Supplement

Methods

MRI Protocols

During a breath-hold of up to 14 seconds, 129Xe gradient recalled echo (GRE) images were acquired with the following settings: TR = 11 ms, TE = 2.7 ms, flip angle = 7°, FOV = 480 x 480 mm^2, matrix = 128 x 128, 9 – 12 slices, thickness = 18 mm, BW = 100 Hz/pixel. For conventional proton MRI, the participant inhaled a 1L bag of UHP N_2 using the same procedures as described above, and a GRE dataset was acquired in a 10 second breath-hold with following settings: TR = 2.87 ms, TE = 1.0 ms, flip angle = 6°, FOV = 480 x 480 mm^2, matrix = 256 x 256, 22 – 28 slices, thickness = 8 mm, BW = 500 Hz/pixel.

Gas dosing and administration

Xe was dosed to 10% of TLC (measured by body plethysmograph). For each administration, the Xe was mixed with ultra high purity N_2 to a total gas dose of 1L. For proton MRI images, the entire 1L dose consisted of N_2. The 1 L gas dose was inhaled from a tedlar bag from end expiration following 2-3 tidal breaths (judged by the gas administrator NM, NK or JHR). Therefore, all images were acquired at a lung volume approximating FRC + 1L.

Results

Xe dosing and lung volumes

The total dose of gas administered was 1L, regardless of participant size. Therefore, the fraction of TLC at which the XeMRI images were obtained differed between participants, but overall was between 80% and 85% on the two testing occasions (Table S1).

Healthy Controls and VDP Threshold Calculation

The healthy normalised voxel intensity distribution was calculated from the mean distribution of 10 healthy children (median age 11, IQR 9.5-12.5). The mean normalised signal intensity was 0.973 units (SD 0.429) (Figure S1). For the linear binning technique, the VDP threshold was derived from this healthy distribution to be 2SD below the mean. Therefore, regions with a normalised signal intensity less than 0.115 units were considered ventilation defects using this analytic technique.

An example of raw XeMRI images from a participant with significant, patchy ventilation defects, along with ventilation defect maps determined using k-means and linear binning techniques, are shown in Figure 2A-D. An example of an intensity histogram of the same participant is shown in Figure 2E, with the healthy distribution overlaid.

Impact of using the highest SNR

Two analyzable image datasets acquired on 23/30 test occasions (76.7%). We assessed the impact of analysing one or more XeMRI images by comparing VDP results generated from the highest SNR image from each test occasion to those generated by averaging all images from each test occasion. This analysis showed no significant difference in the primary outcome between these approaches (Table S1). The mean SNR of the 30 analyzed images was 45.1 (range 11.7, 82.2) and the mean SNR of the excluded 23 images was 36.3 (range 15.6, 80.3). In order to minimize the potential impact of low SNR on VDP calculation (1), the primary analysis was performed on the single image (highest SNR) dataset.

MBW Postural Dependence

MBW testing was performed in both the seated and supine postures on both test occasions for all participants. Overall, LCI_{supine} was significantly higher than $LCI_{sitting}$ (mean difference 0.7 units; 95%CI 0.2, 1.2; p=0.008) but this difference was driven by data from post-treatment tests, with significant postural changes in LCI only seen after treatment (Table S2). Within subjects, the average postural LCI change was greater on

the post-treatment test occasion than on the pre-treatment test occasion (mean difference 0.9 units; 95%CI 0.2, 1.7; p=0.01). In other words, LCI increased more when transitioning from the seated to the supine position after treatment than it did before treatment.

The posture-dependence of the components of LCI (LCI=cumulative expired volume [CEV]/functional residual capacity [FRC]) were inspected individually. FRC_{supine} was significantly lower than $FRC_{sitting}$ both before and after treatment (Table S2). Within-subjects, this postural dependence was enhanced after antibiotic treatment, with FRC dropping 0.12L further (95%CI -0.24, -0.01; p=0.003) with a shift to the supine position on post-treatment test occasions compared to pre-treatment test occasions. No such relationship was seen with CEV, suggesting that the postural change in LCI was driven mostly by a change in the FRC.

MRI-physiology correlation

Significant correlations were observed between VDP (k-means and histogram techniques) and LCI, FEV_1 and RV:TLC (Table S3). Correlation of k-means and linear binning VDP values with seated LCI (R^2=0.38 and 0.36 respectively) was higher than with supine LCI (R^2=0.21 and 0.18 respectively). Correlation of FEV_1 and RV:TLC with K-means VDP (R^2=0.30 and 0.34 respectively) was higher than with the linear binning VDP (R^2=0.17 and 0.15 respectively).

Table S1 – Median (IQR) plethysmographic lung volumes of patients measured at the pre- and post-treatment scans. The fractional imaging volume represents the percent of total lung capacity (TLC) at which the imaging was performed.

	Pre-treatment	**Post-treatment**
TLC (L)	3.78 (3.52, 5.25)	4.00 (3.75, 4.8)
FRC_{pleth} (L)	2.41 (2.00, 3.06)	2.20 (2.01, 2.75)
^{129}Xe dose (mL)	380 (350, 530)	400 (380, 480)
Imaging volume (L)	3.41 (3.00, 4.06)	3.20 (3.01, 3.75)
Fractional imaging volume (%)[1]	84.6 (79.0, 88.5)	79.5 (75.1, 83.7)

[1](FRC+1)/TLC x 100%

Table S2 – Sensitivity analysis of using the highest SNR image or the average of all interpretable images. *denotes statistical significance p<0.05.

	Pre-treatment; mean (SD)	**Post-treatment; mean (SD)**	**Within subject absolute change; mean (95%CI)**	**Within-subject relative change (%); mean (95%CI)**
Highest bag only				
VDP (%; LB)	6.4 (3.8)	3.4 (2.9)	-3.0 (-5.0, -1.0)*	-44.2 (-60.2, -28.3)*
VDP (%: k-means)	10.4 (4.5)	6.7 (4.1)	-3.8 (-5.9, -1.7)*	-34.6 (-49.3, -19.9)*
Mean of all bags				
VDP (%; LB)	6.6 (3.9)	3.7 (2.7)	-2.8 (-4.1, -1.5)*	-38.3 (-49.4, -27.1)*
VDP (%; k-means)	10.6 (4.6)	6.9 (4.5)	-2.6 (-3.9, -1.2)*	-33.3 (-44.9, -21.8)*

Table S3 – Postural dependence of MBW outcomes, stratified by pre- and post-treatment test occasions. Difference between supine and seated MBW outcomes are shown from all visits as well as isolated to pre- and post-treatment visits. The within-subject mean change of the supine-sitting difference is shown in the last column. Data are displayed as mean difference (95%CI). *denotes that the mean difference is significantly different from 0 ($p<0.05$).

	Supine – seated postural difference, by test occasion			**Within-subject change in postural difference after treatment**
	Overall	**Pre-treatment only**	**Post-treatment only**	
LCI2.5	0.7 (0.2, 1.2)*	0.2 (-0.5, 0.9)	1.2 (0.5, 1.8)*	0.9 (0.2, 1.7)*
FRC (L)	-0.25 (-0.31, -0.17)*	-0.18 (-0.28, -0.08)*	-0.30 (-0.40, -0.20)*	-0.12 (-0.24, -0.01)*
CEV (L to achieve the 2.5% threshold)	-2.1 (-4.0, -0.1)*	-2.5 (-5.2, 0.2)	-1.6 (-4.6, 1.3)	0.9 (-1.5, 3.2)

Table S4 – MRI-physiology correlation. Results of linear regression of XeMRI outcome measures (k-means VDP, Histogram VDP) with MBW, spirometry and plethysmography outcomes. Data are shown as R^2 and p-value for significance of association. *denotes a significant correlation ($p<0.05$).

	LCI (seated)	**LCI (supine)**	**FEV1 (%)**	**RV/TLC**
K-means	0.38*	0.21*	0.30*	0.34*
Linear binning	0.36*	0.18*	0.17*	0.15*

Supplemental Figures

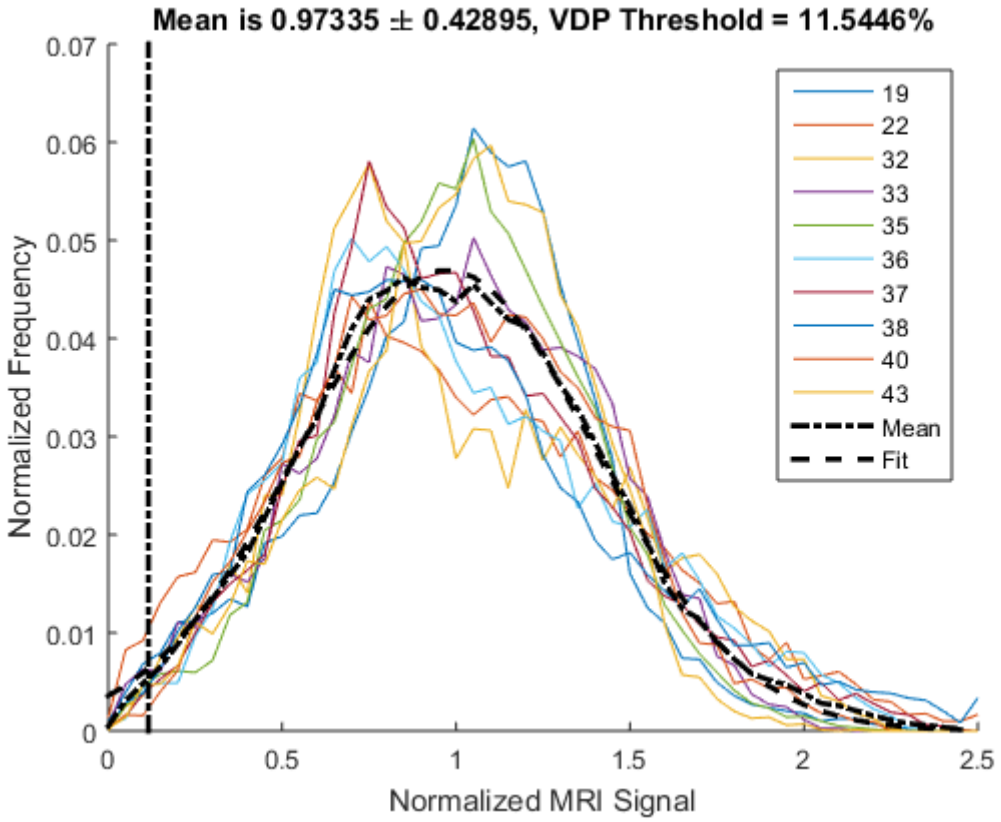

Figure S1 – Normalised voxel signal intensity histograms for all healthy subjects. The voxel intensity distribution for all healthy subjects with an overlaid mean (dot/hash line) and fit (dash line) curves is shown. The vertical line represents the VDP threshold that was established from this distribution.

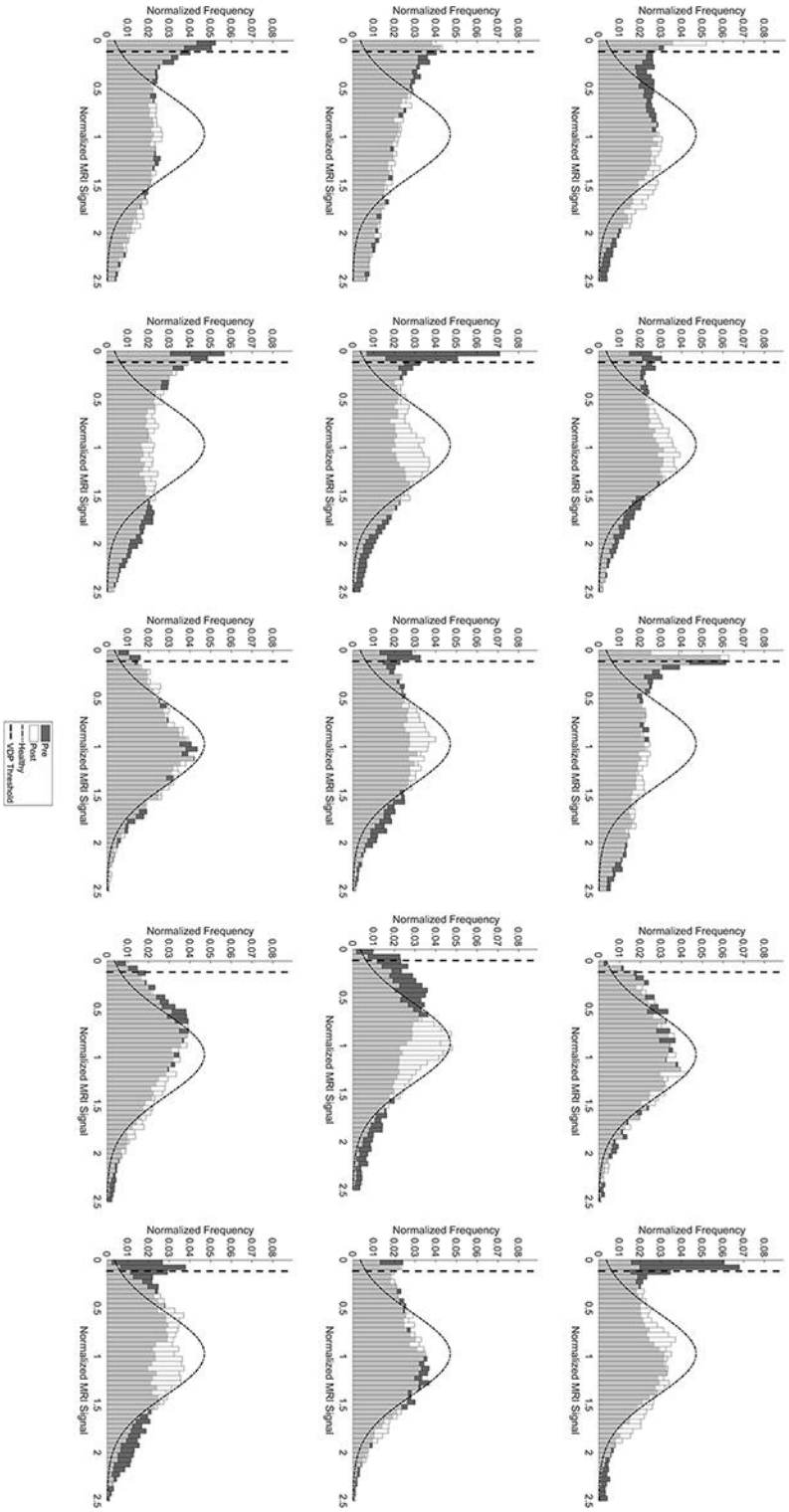

Figure S2 – Normalized voxel signal intensity histograms for all CF subjects before and after therapy. Pre-treatment distribution is shown in dark grey and post-treatment distribution is shown in white. Healthy distributions are overlaid in a hashed black curve and the ventilation defect threshold is identified with a dashed vertical line.

References

1. He M, Tan F, Rankine L, Fain S, Driehuys B. The Effect of Signal to Noise Ratio on Linear-binning and Adaptive k-means Quantification of Hyperpolarized Xe Ventilation MRI. ISMRM. Paris, FRA; 2018.